AFWAL-TR-85-4110

FRACTURE MECHANICS OF MULTIPLE CRACK INITIATIONS

AN APPLICATION FOR FRACTURE MECHANICS ANALYSES OF GAS TURBINE ENGINE DISKS

B. A. Cowles, A. B. Thakker, G. E. King
United Technologies Corporation
Pratt & Whitney
Engineering Division
P.O. Box 2691, West Palm Beach, Florida 33402

October 1985

Interim Report for Period February 1981 to June 1983.

Approved for public release; distribution unlimited.

Materials Laboratory
Air Force Wright Aeronautical Laboratories
Air Force Systems Command
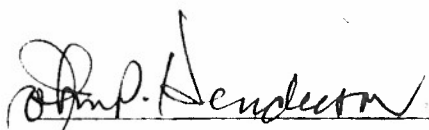Wright-Patterson Air Force Base, Ohio 45433

NOTICE

When Government drawings, specifications, or other data are used for any purpose other than in connection with a definitely related Government procurement operation, the United States Government thereby incurs no responsibility nor any obligation whatsoever; and the fact that the government may have formulated, furnished, or in any way supplied the said drawings, specifications, or other data, is not to be regarded by implication or otherwise as in any manner licensing the holder or any other person or corporation, or conveying any rights or permission to manufacture, use, or sell any patented invention that may in any way be related thereto.

This report has been reviewed by the Office of Public Affairs (ASD/PA) and is releasable to the National Technical Information Service (NTIS). At NTIS, it will be available to the general public, including foreign nations.

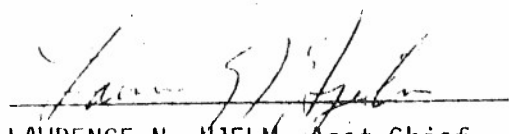This technical report has been reviewed and is approved for publication.

JOHN P. HENDERSON, Chief
Metals Behavior Branch
Metals and Ceramics Division

BRYAN H. FORTSON, 1Lt, USAF
Project Engineer
Metals Behavior Branch

FOR THE COMMANDER:

LAWRENCE N. HJELM, Asst Chief
Metals and Ceramics Division
Materials Laboratory

REPORT DOCUMENTATION PAGE

1a. REPORT SECURITY CLASSIFICATION UNCLASSIFIED	1b. RESTRICTIVE MARKINGS None

2a. SECURITY CLASSIFICATION AUTHORITY	3. DISTRIBUTION/AVAILABILITY OF REPORT
2b. DECLASSIFICATION/DOWNGRADING SCHEDULE	Approved For Public Release; Distribution Unlimited

4. PERFORMING ORGANIZATION REPORT NUMBER(S)	5. MONITORING ORGANIZATION REPORT NUMBER(S)
P&W/ED FR-18778	AFWAL-TR-85-4110

6a. NAME OF PERFORMING ORGANIZATION United Technologies Corporation Pratt & Whitney Engineering Division	6b. OFFICE SYMBOL (If applicable)	7a. Air Force Wright Aeronautical Laboratories Air Force Systems Command Materials Laboratory
6c. ADDRESS (City, State and ZIP Code) P.O. Box 2691 West Palm Beach, FL 33402		7b. ADDRESS (City, State and ZIP Code) AFWAL/MLLN Wright-Patterson AFB, Ohio 45433

8a. NAME OF FUNDING/SPONSORING ORGANIZATION	8b. OFFICE SYMBOL (If applicable)	9. PROCUREMENT INSTRUMENT IDENTIFICATION NUMBER F33615-80-C-5160

8c. ADDRESS (City, State and ZIP Code)	10. SOURCE OF FUNDING NOS.			
	PROGRAM ELEMENT NO.	PROJECT NO.	TASK NO.	WORK UNIT NO.
	DARPA 3993			

11. TITLE (Include Security Classification)
Fracture Mechanics of Multiple Crack Initiations

12. PERSONAL AUTHOR(S)
B.A. Cowles, A.B. Thakker, G.E. King

13a. TYPE OF REPORT Interim	13b. TIME COVERED FROM 2-81 TO 6-83	14. DATE OF REPORT (Yr., Mo., Day) 1985 October	15. PAGE COUNT 43

16. SUPPLEMENTARY NOTATION

17.	COSATI CODES		18. SUBJECT TERMS (Continue on reverse if necessary and identify by block number)
FIELD	GROUP	SUB. GR.	

19. ABSTRACT (Continue on reverse if necessary and identify by block number)

The capability of an existing design approach and a new multiple-degree-of freedom model for predicting crack growth lives in engine components, subject to multiple crack initiations, was investigated.

It was determined that the existing design approach, which is based on modified stress intensities for interacting cracks, and a newly developed multiple degree-of-freedom model, adequately predict crack growth lives for multiple crack initiations under the conditions tested. These conditions reflect current gas turbine engine Retirement-for-Cause applications.

20. DISTRIBUTION/AVAILABILITY OF ABSTRACT UNCLASSIFIED/UNLIMITED ☐ SAME AS RPT. X DTIC USERS ☐	21. ABSTRACT SECURITY CLASSIFICATION UNCLASSIFIED

22a. NAME OF RESPONSIBLE INDIVIDUAL	22b. TELEPHONE NUMBER (Include Area Code)	22c. OFFICE SYMBOL

DD FORM 1473, 83 APR   EDITION OF 1 JAN 73 IS OBSOLETE.

FOREWORD

This interim report documents work conducted as a task entitled "Fracture Mechanics of Multiple Crack Initiations (No. 132)" under the Air Force Wright Aeronautical Laboratories Engine Component Retirement for Cause Contract, No. F33615-80-C-5160, with the Project Number assigned as DARPA 3993. This is an ongoing contract effort. This report is published in compliance with the Contract Data Requirements List and describes the technical accomplishments of the Multiple Crack Initiation Fracture Mechanics Task.

The Air Force RFC Program Manager is Dr. W. H. Reimann, and the Project Engineer is 1st Lt. R. Sincavage, both of the Air Force Wright Aeronautical Laboratories, Metals Behavior Branch of the Materials Laboratory (AFWAL/MLLN). The program is conducted by the Materials Engineering and Technology Laboratories of Pratt & Whitney, Engineering Division/Florida Operations (P&W/ED FO), West Palm Beach, Florida. The Project Engineer is R. White and the Program Manager is J. A. Harris, Jr., reporting through M. C. VanWanderham, Manager, Mechanics of Materials and Structures.

The Engine Component Retirement for Cause (RFC) program is jointly sponsored by the Materials Sciences Office, Defense Advanced Research Projects Agency (DARPA), and the Materials Laboratory, Air Force Wright Aeronautical Laboratories. DARPA and the U.S. Air Force participant's contributions to the program and to the work reported herein are acknowledged and appreciated.

2013C

TABLE OF CONTENTS

LIST OF ILLUSTRATIONS

LIST OF ILLUSTRATIONS (Continued)

LIST OF TABLES

2472C

SECTION I

INTRODUCTION

RETIREMENT FOR CAUSE BACKGROUND

Historically, methods used for predicting the life of gas turbine engine rotor components have resulted in a conservative estimate of useful life. Most rotor components are limited by low-cycle fatigue (LCF) generally expressed in terms of mission equivalency cycles or engine operational hours. When some predetermined life limit is reached, components are retired from service.

Total fatigue life of a component consists of a crack initiation phase and a crack propagation phase. Engine rotor component initiation life limits are analytically determined using lower bound LCF characteristics. This is established by a statistical analysis of data indicating the cyclic life at which 1 in 1000 components, such as disks, will have a fatigue induced crack of approximately 0.030-inch surface length. By definition then, 99.9 percent of the disks are being retired prematurely. It has been documented that many of the 999 remaining retired disks have considerable useful residual life. Under the RFC philosophy, each of these disks could be inspected and returned to service. The return-to-service (RTS) interval is determined by a fracture mechanics calculation of remaining propagation life from a crack just small enough to have been missed during inspection. This procedure could be repeated until the disk has incurred measureable damage, at which time it is retired for that reason (cause). RFC is a methodology under which and engine component would be retired from service when it had incurred quantifiable damage, rather than because an analytically determined minimum design life had been reached.

The Materials and Aero Propulsion units of the Air Force Wright Aeronautical Laboratories (AFWAL) have been conducting in-house research and development activities in the RFC area since 1972. A joint study by the Metals Behavior Branch (AFWAL/MLLN), the Engine Assessment Branch (AFWAL/POTA), and the Directorate of Engineering, Aeronautical Systems Division (Reference 1) was undertaken in 1975 to assess the state of the art of the technologies involved in RFC. This study addressed and used a TF33 3rd-stage turbine disk as a demonstration vehicle. As a result of this study, the technical requirements for implementing an RFC approach were identified. These technology requirements fell into four areas: stress analysis, crack growth analysis, nondestructive evaluation (NDE), and mechanical testing. Pratt & Whitney had also begun extensive research and development programs under corporate, Independent Research and Development (IR&D), and Government contract sponsorship in 1972 to identify and develop the applied fracture mechanics and NDE technologies necessary to realize the RFC concept. In addition to the technical areas defined by the efforts discussed above, the broad areas of economics and logistics management also must be incorporated and integrated before RFC could become a viable, implementable maintenance concept for managing life limited gas turbine engine components.

The culmination of these preliminary activities was a study conducted by Pratt & Whitney Engineering Division, Florida Operations (P&W/ED FO) from 1979 to 1980 under Defense Advanced Research Projects Agency (DARPA) and AFWAL sponsorship entitled "Concept Definition: Retirement for Cause of F100 Rotor Components" (Reference 2). This program was the first to consolidate and focus these disciplines on a specific engine system and to quantify the benefits and risks involved (Reference 3). Upon completion of the initial Concept Definition Study, AFWAL/Materials Laboratory established a major thrust in RFC with the goal of reducing the concept to practice with first system implementation to occur in early 1986 on the F100 engine at the San Antonio Air Logistics Center (SA-ALC). P&W/ED FO is developing the

20140

probabilistic life analyses, and integrated logistics/economic methodology to support this implementation.

FRACTURE MECHANICS OF MULTIPLE INITIATIONS

The studies previously referenced have cited the importance of accurate crack growth analyses in enabling the RFC concept to be implemented with confidence. As a part of the ensuing "Engine Component Retirement for Cause" contract program, several areas of concern in conducting crack growth analyses of gas turbine engine components were identified. Included in those concerns was the impact that a multiplicity of fatigue crack initiations might have on crack growth predictions. The observed tendency for some materials is to develop fatigue cracks from multiple origins, depending on service environment, geometry, and surface condition of the material.

Current crack growth predictions for most engine component critical locations are based on singularly initiating and propagating cracks. The propensity for multiple initiations is addressed by specific assumptions of crack geometry, such as through-crack versus surface or corner geometry, variable crack aspect ratio, and interactions with other nearby critical locations. These assumptions are reviewed individually for each prediction case. The assumptions are supported where possible by component testing and by service experience in rare cases where data are available.

The objective of this report was to experimentally produce and quantify the effects of multiple, interacting cracks for materials and conditions relevant to the RFC program, and to assess their impact on crack growth predictions relevant to the program.

SECTION II

OBJECTIVE AND APPROACH

Applied fracture mechanics is predicated on a uniparametric relationship between the status of the stress field surrounding a crack (as expressed by K, the stress intensity factor) and the dynamic response of a crack, da/dN. Currently available *handbook* solutions for K have proven to be adequate for nearly all singly occurring cracks. In real components, however, several cracks may initiate more or less simultaneously within a stress concentration area (e.g., bolthole, slot), then synergistically propagate toward linkup and subsequently behave as a single macrocrack. Only after linkup can these be addressed in the conventional manner.

This study investigated current methods for multiple crack growth life prediction and was structured to suggest a modified model, if necessary. The problem of multiple crack initiation, linkup, and propagation is nearly intractable with analytical treatments, which must characterize material response to a perturbation within an idealized stress field. Application of fracture mechanics techniques to geometries experiencing crack multiplicity necessitates an experimental determination of the behavior of synergistically propagating fatigue cracks and an engineering method for predicting their behavior.

The objective of this task was to determine whether multiple cracking would significantly affect life prediction requirements for RFC purposes. Alloys, test conditions, and geometries were selected specifically to address RFC applications.

To experimentally quantify the behavior of multiple cracks, the technical effort consisted of:

1. Laboratory investigation of multiple crack interaction

2. Assessment of current approximate treatments of the problem

3. Modification of experimental/empirical models to describe the behavior of multiple-originating, synergistically propagating cracks if required.

The technical approach consisted of three steps. First, a variety of potentially interacting small fatigue cracks were initiated in notched specimens. These cracks were then grown at selected stresses and temperatures until complete failure occurred. Using several techniques, crack sizes were periodically measured to compliment post-test crack front measurements. Finally, results were analyzed on a remaining life basis; that is, measured remaining-life from a predetermined crack size to failure was compared with predicted remaining life.

This program was not intended to provide an exhaustive evaluation of fracture mechanics of multiple initiations. It was focused on materials and loading conditions relevant to RFC rotor (disks and spacers) components of tactical fighter engines, and to assess effects of multiple initiations on the accuracy of fracture mechanics based life predictions for that application.

2014C

SECTION III

MATERIAL SELECTION

Waspaloy and Ti 6-2-4-6 were the two materials chosen for the program; both of which have demonstrated a tendency to develop multiple cracks under low-cycle fatigue conditions.

Waspaloy is a precipitation hardenable nickel-based superalloy offering good strength and corrosion resistance at elevated temperatures. It is used extensively for rotating disks and seals in aircraft gas turbine engines. The alloy was conventionally forged from ingot to a disk/pancake configuration suitable for this study. Nominal composition and heat treatment for Waspaloy are presented in Table 1. Resultant microstructure of the material is presented in Figure 1.

TABLE 1.

NOMINAL COMPOSITION AND HEAT TREATMENT FOR WASPALOY

Chemical Composition	Required
Carbon	0.02 to 0.10
Manganese	0.75 max
Sulfur	0.020 max
Silicon	0.75 max
Chromium	18.0 to 21.0
Cobalt	12.0 to 15.0
Molybdenum	3.5 to 5.0
Titanium	2.75 to 3.25
Aluminum	1.20 to 1.60
Zirconium	0.02 to 0.12
Boron	0.003 to 0.010
Iron	2.0 max
Copper	0.10 max
Bismuth	0.5 ppm max
Lead	10 ppm max
Nickel	Balance

Heat Treatment:

1010°C to 1038°C/4/OQ	1016°C/4/OQ
843°C/4/AC	843°C/4/AC
760°C/16/AC	760°C/16/AC

2014C

The titanium, Ti 6Al-2Sn-4Zr-6Mo, is a heat-treatable alpha-beta alloy which provides high tensile and creep strengths and LCF capability for applications up to approximately 427°C (800°F). Ti 6-2-4-6 is used for disks and seals in the fan and forward stages of the high-pressure compressor of gas turbine engines. Nominal composition and heat treatment for Ti 6-2-4-6 are presented in Table 2; typical microstructure is shown in Figure 2.

4

FD 283903

500X

100X
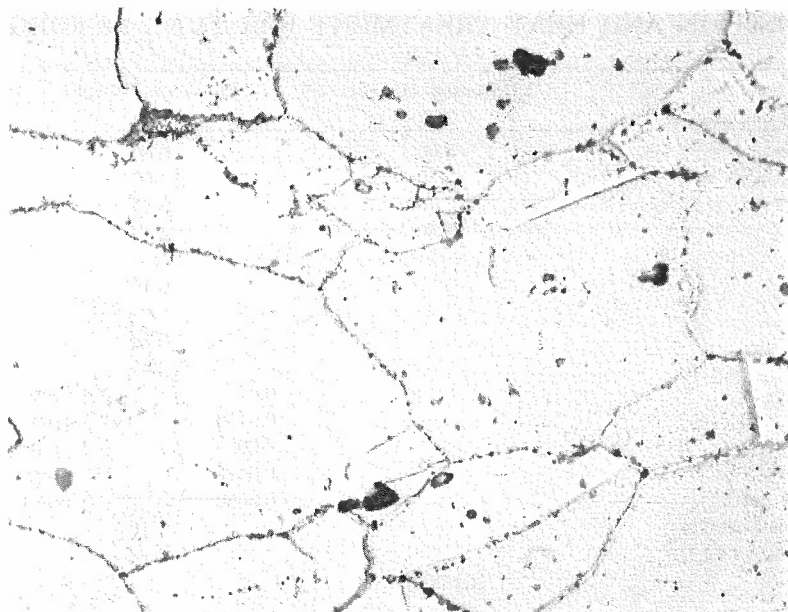
Figure 1. Typical Optical Microstructure for Waspaloy

TABLE 2.

CHEMICAL COMPOSITION AND HEAT TREATMENT FOR TI 6-2-4-6 FORGINGS

Chemical Composition	Minimum Weight (%)	Maximum Weight (%)	
Aluminum	5.50	6.50	
Zirconium	3.50	4.50	
Tin	1.75	2.25	
Molybdenum	5.50	6.50	
Silicon	—	0.10	
Iron	—	0.15	
Carbon	—	0.04	
Copper (3.2.1)	—	0.10	
Oxygen	—	0.15	
Nitrogen	—	0.04	(400 ppm)
Hydrogen	—	0.0150	(150 ppm)
Boron	—	0.003	(30 ppm)
Yttrium, rotor parts (4.2.1)	—	0.0010	(10 ppm)
Yttrium, nonrotor parts	—	0.0050	(50 ppm)
Other elements, each (3.2.1)	—	0.10	
Other elements, total (3.2.1)	—	0.40	
Titanium	Remainder		

Heat Treatment:

1690°F ± 15 (921°C ± 8.3)/2 hr	—	Fan air cool to 700°F (371°C)
1525°F ± 15 (829°C ± 8.3)/2 hr	—	Water quench
1100°F ± 15 (593°C ± 8.3)/8 hr	—	Air cool

2014C
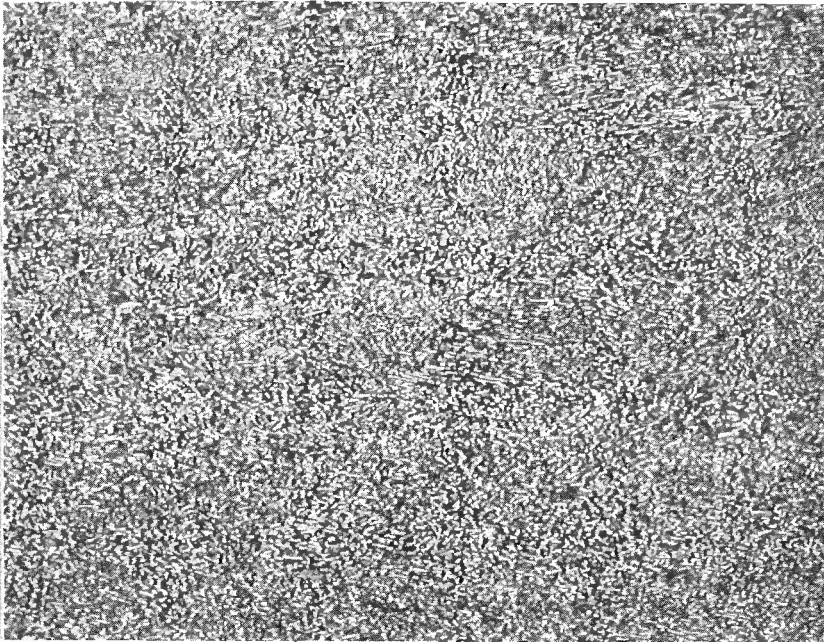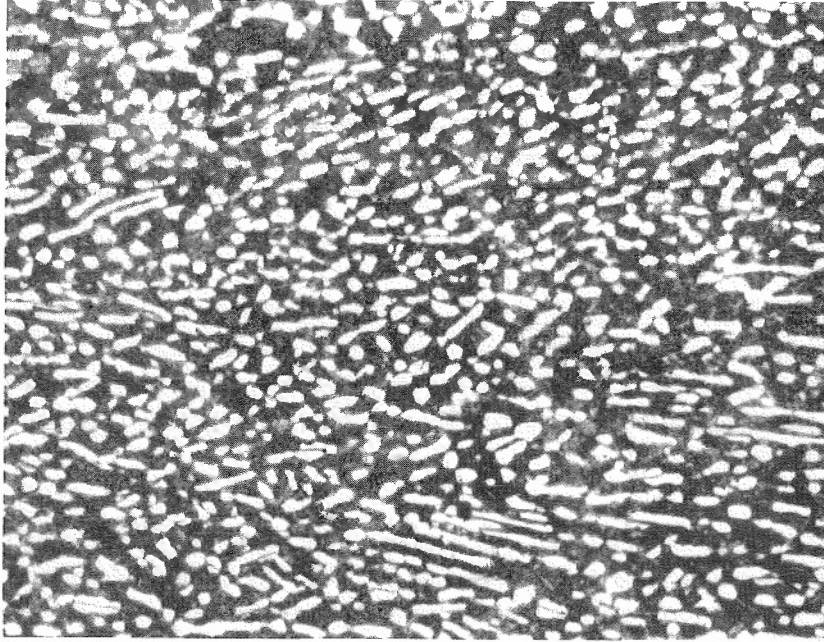
500X

100X

FD 283904

Figure 2. Typical Optical Microstructure for Ti 6-2-4-6

7

SECTION IV

EXPERIMENTAL PROGRAM AND RESULTS

TEST SPECIMEN AND EXPERIMENTAL METHODS

The experimental program used the double notch specimen (Figure 3). This specimen exhibits a varying stress field that is representative of typical engine component locations (for example, disk live rim). It has been extensively characterized and the stress critical notch area is accessible for visual and other NDE inspections. For both materials, the specimen blanks were machined from pancake forgings with the longest direction coincident with the tangential orientation.

All tests including precrack cycles to sharpen the EDM starter flows were conducted using closed loop electrohydraulic servo-controlled test machines (Figure 4) operating in load control mode with a sawtoothed load cycle. For Waspaloy, a clamshell, resistance type furnace was used to attain the 400°F test temperature. Thermocouples attached to the specimen surface were used to monitor and control temperature.

To facilitate early detection of microcracks, a special eddy current probe was constructed by P&W (Figure 5). The spring-loaded probe was made to closely fit the groove geometry and to maintain the same contact force during sweeps from edge-to-edge. Attempts to use acoustic emission for detecting initiation were discontinued due to excessive background noise.

Detection of early cracking for both the naturally initiated and preflawed specimens was documented by two methods: 1) white-light inspection with a telemicroscope and 2) acetate film replication. Both methods are performed with the test specimen under tensile load. These inspections were performed at the outset and periodically throughout the test.

In addition to acetate film replication, a multiple heat tinting technique was used to monitor crack progression. The procedure established for each alloy allowed three discernible zones while keeping tinting temperatures low enough to ensure no subsequent influence on crack growth. Each tint cycle lasted 2 hours and was applied in the test rig at 20 percent of maximum test load to facilitate oxidation. Post test fractography was used to correlate crack propagation results from tinting and replication. A typical tinted fracture surface for Waspaloy is shown in Figure 6.

TEST MATRIX AND CONDITIONS

The experimental program addressed seven crack cases: singular surface, singular corner, and five multiple crack conditions combining surface and corner cracks of different sizes and spacing. In most specimens, starter flaws were introduced using controlled Electrical Discharge Machining (EDM) notches. The use of preflaws allowed control of flaw locations, shapes (various aspect ratios), and the number of initiation sites. The matrix of flaw shapes and their dimensions are shown in Figure 7. The remaining specimens were tested in the *as-machined* condition to obtain naturally initiated cracks. A matrix of tests by material, type of starter flaw, and location is presented in Table 3.

$(K_T = 2.18)$

Section A-A
(Enlarged 2X)

0.252
0.248

See Note 4

0.362   0.258
0.358   0.254

C$_L$ 0.500 Dia Ref

0.054
0.050   Rad, 2 Places (See Notes 1, 3, 4)

C$_L$ — A

— A

1.020
0.980   Rad, 4 Places

0.500-20UNJF-3A
Both Ends

0.380
0.370

0.380
0.370
0.520
0.480   Rad, 4 Places

Center Holes
Permitted

Gage Section

Ident Mark
Per Note 5

C$_L$
3.020
2.980
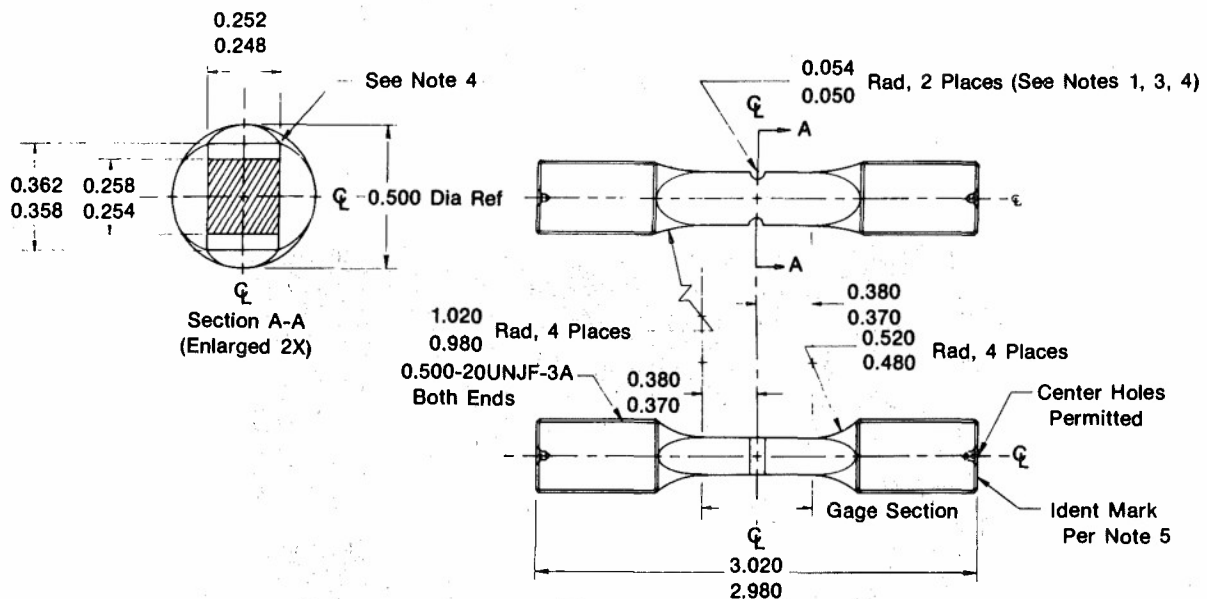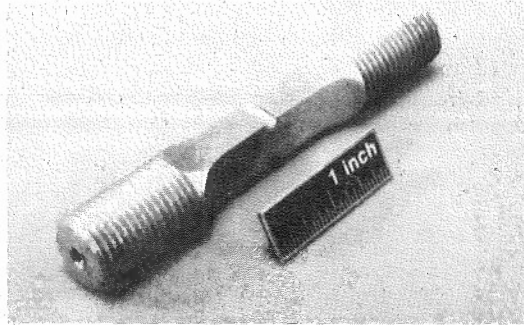
All Dimensions Are in Inches

1   Semicircular Notch (0.052) Radii To Be Ground with 320 Grit Wheel

2   Grind Finish Gage Section. Polish Gage Section (Including Notches) in Longitudinal Direction to 8 RMS Microinch Finish or Better, with All Edges Rounded to 0.010-0.015 Radius

3   Semicircular Notch C$_L$'s Must Be Parallel with Each Other Within 0.002 FIR, and Located Within 0.002 of Gage Section Transverse C$_L$

4   Flat Faces of Gage Section and Notch Bottoms Must Be Symmetric Within 0.002 FIR

5   Identification Markings Permitted Only on Ends of Specimen

FD 248371

Figure 3.   Double Notch LCF Test Specimen

9
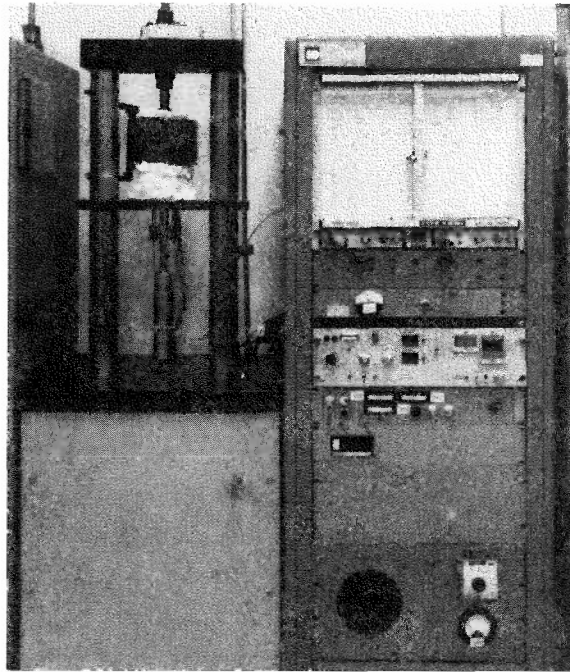
KFAE 215490

Figure 4. Servohydraulic Closed-Loop LCF Test Machine
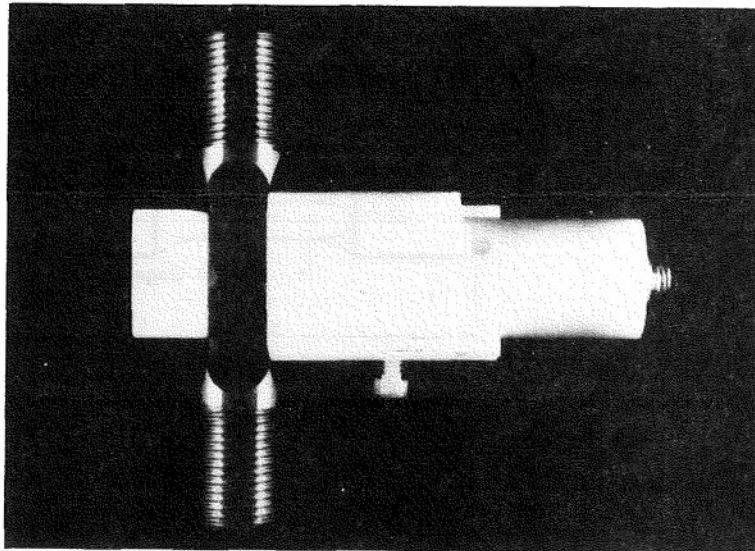
FD 248383

Figure 5. Double Notch Specimen and Eddy Current Probe Assembly

Test conditions were selected to be representative of the Waspaloy and Ti 6-2-4-6 gas turbine engine applications. Waspaloy tests were conducted at 400°F, 10 cycles per minute (cpm), and a stress ratio (R) of 0.05. Two maximum stress conditions were tested: 110,000 and 96,000 pounds per square inch (psi). Initial Ti 6-2-4-6 tests were performed at room temperature (RT), 10 cpm, stress ratio of 0.05, with a maximum stress of 92,000 psi. Although representative of the more severe usage conditions for the material, no interaction of multiple cracks occurred at this stress level. The maximum stress level for Ti 6-2-4-6 was later reduced to 50,000 psi to allow interaction of multiple cracks for the purposes of this task.
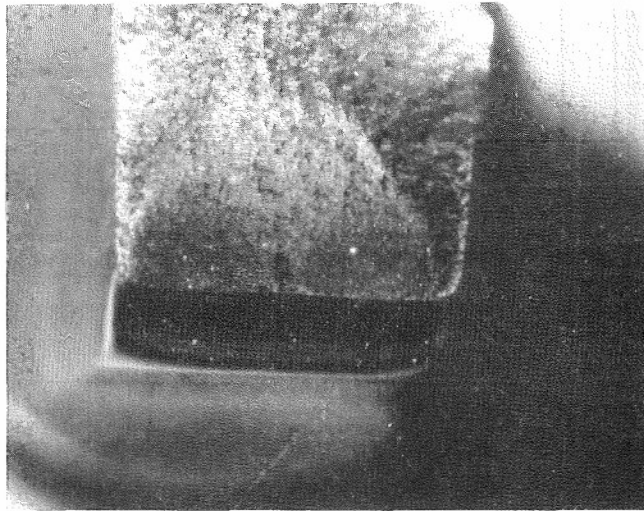
Side "B"
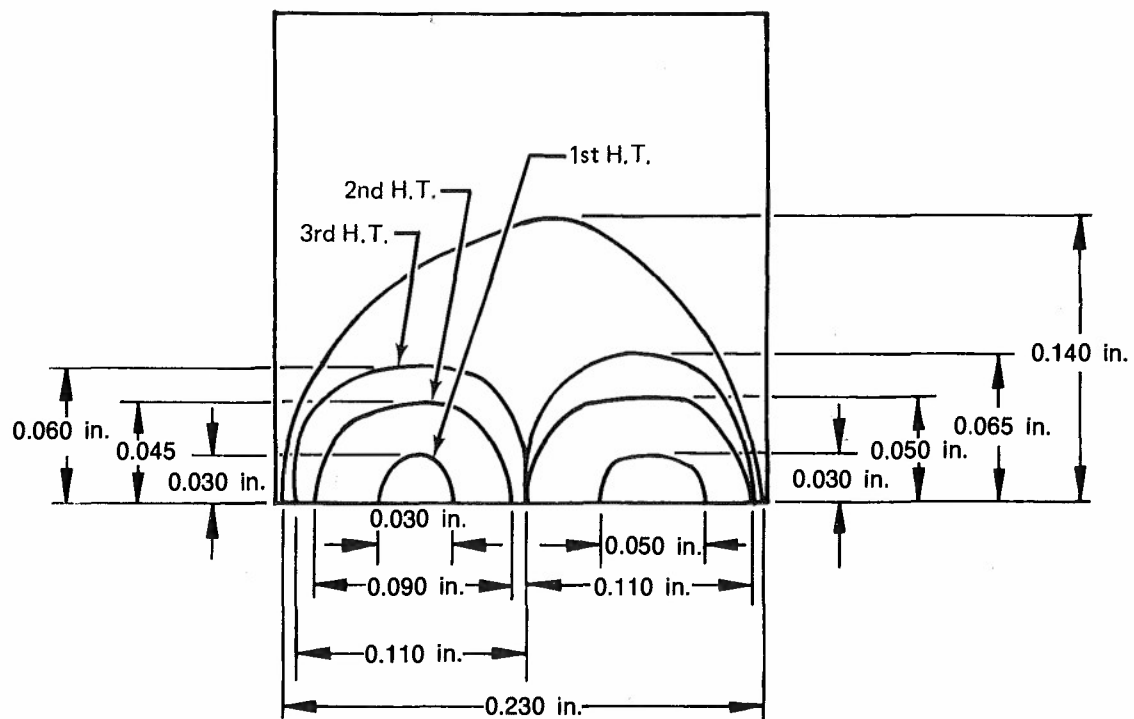
FD 267085

Figure 6. Typical Heat Tint Zones on Waspaloy Fractured Double Notch Specimen

11

Singular Surface Crack

Singular Corner Crack

Case 1 Two Equal Noninteracting Surface Cracks (Shallow)

Crack Plane

Note: Dimensions in Inches (Nominal)

Case 2 Two Interacting Cracks (Equal Size)

Double Notch Specimen

Case 3 Two Nonsymmetric. Noninteracting Cracks

Case 4 Corner and Surface Crack Combination (Interacting)

Case 5 Three Noninteracting Surface Cracks (Deep)

Figure 7. Fracture Mechanics of Multiple Initiations — Matrix of Flaw Shapes

FD 248360

12

TABLE 3.

TEST MATRIX

	Naturally Initiated	Eloxed Singular Crack		Eloxed Multiple Cracks				
		Corner	Surface	Case 1	Case 2	Case 3	Case 4	Case 5
	Waspaloy (PWA 1016) (400°F)							
Stress Level $\sigma_1 = 96$ ksi	2	1	1	1	1	1	1	1
Stress Level $\sigma_2 = 110$ ksi	2	2	2	2	2	2	2	2
	Titanium 6-2-4-6 (PWA 1216) (R.T.)							
Stress Level $\sigma_1 = 92$ ksi	2	1	1	1	1	1	1	1
Stress Level $\sigma_2 = 50$ ksi	—	—	—	1	1	1	1	1

2014C

RESULTS

All specimens were cycled, under the test conditions described earlier, to fracture. Failure lives are summarized by specimen configuration and starting flaw size in Tables 4 and 5, and plotted in Figures 8 and 9. Crack length and depth data obtained from replication and heat tinting were combined to generate crack front progression data. Representative graphic illustrations of crack nucleation, progression, link-up, and failure for each condition tested are shown in Figures 10 through 16 for Wasploy and Figures 17 through 23 for Ti 6-2-4-6. Included with each illustration is a tabulation of crack width and depth versus cycles. To eliminate effects of variable cycle times to develop actively growing cracks from the EDM preflaws, all analyses were performed based on remaining life from selected crack sizes.

TABLE 4.

CYCLES TO FAILURE FOR MULTIPLE CRACK WASPALOY DOUBLE NOTCH SPECIMENS

$T = 400°F$, $R_\sigma = 0.05$, $f = 10$ cpm

Specimen Number	Max Stress Level (ksi)	Actual Crack Size Width × Length (in.)	Cycles to Failure
Surface Flaw			
Nominal Dimensions		0.040 × 0.020	
5	96	0.039 × 0.018	17,204
8	110	0.038 × 0.020	7,336
14	96	0.033 × 0.017	17,424
Corner Flaw			
Nominal Dimensions		0.025 × 0.025	
10	110	0.022 × 0.026	15,013
11	110	0.023 × 0.035	12,436
12	96	0.028 × 0.025	19,680
15	96	0.020 × 0.015	20,533
Case No. 1 Two Non-Interacting Surface Flaws			
Nominal Dimensions		0.04 × 0.015/0.04 × 0.015	
1A	96	0.042 × 0.01/0.044 × 0.015	15,513
17	110	0.040 × 0.008/0.040 × 0.010	12,455
18	110	0.040 × 0.01/0.040 × 0.012	9,306
Case No. 2 Two Interacting Suface Flaws			
Nominal Dimensions		0.04 × 0.015/0.04 × 0.015	
4A	96	0.04 × 0.017/0.04 × 0.015	15,264
3A	110	0.04 × 0.016/0.04 × 0.015	8,022
7A	110	0.04 × 0.016/0.04 × 0.015	6,372
Case No. 3 Two Non-Symmetric Noninteracting Surface Flaws			
Nominal Dimensions		0.04 × 0.015/0.06 × 0.015	
10A	96	0.043 × 0.015/0.061 × 0.018	13,578
8A	110	0.045 × 0.017/0.06 × 0.018	10,039
9A	110	0.040 × 0.015/0.055 × 0.016	6,430
Case No. 4 Surface and Corner Crack Combination			
Nominal Dimensions		0.04 × 0.015/0.02 × 0.02	
15A	96	0.039 × 0.022/0.016 × 0.021	11,073
13A	110	0.037 × 0.016/0.013 × 0.015	8,248
14A	110	0.035 × 0.019/0.014 × 0.019	8,853
Case No. 5 Three Symmetric Noninteracting Surface Cracks			
Nominal Dimensions		0.02 × 0.01/0.02 × 0.01/0.02 × 0.01	
17A	110	0.02 × 0.008/0.018 × 0.009/0.017 × 0.01	9,955
16A	96	0.018 × 0.01/0.17 × 0.01/0.016 × 0.01	14,966
19A	110	0.019 × 0.008/0.018 × 0.009/0.018 × 0.01	7,352

14

TABLE 5.

CYCLES TO FAILURE FOR MULTIPLE CRACK TI 6-2-4-6 DOUBLE NOTCH SPECIMENS

NOMINAL STRESS = 50 ksi, R_σ = 0.05, T = 70°F, f = 10 cpm

Specimen Number	Case Number	Initial Flaw Size Width × Depth (in.)	Cycles to Failure
8B	1 Non-Interacting Surface Flaw	0.040 × 0.014/0.040 × 0.014	9,987
10B	2 Two-Interacting Surface Flaws	0.048 × 0.020/0.048 × 0.015	5,958
12B	3 Non-Symmetric Non-Interacting	0.041 × 0.014/0.060 × 0.015	7,091
14B	4 Corner/Surface Combination	0.018 × 0.020/0.039 × 0.014	11,920
16B	5 Three Symmetric Non-Interacting	0.020 × 0.010/0.020 × 0.011 0.020 × 0.011	11,167

2014C
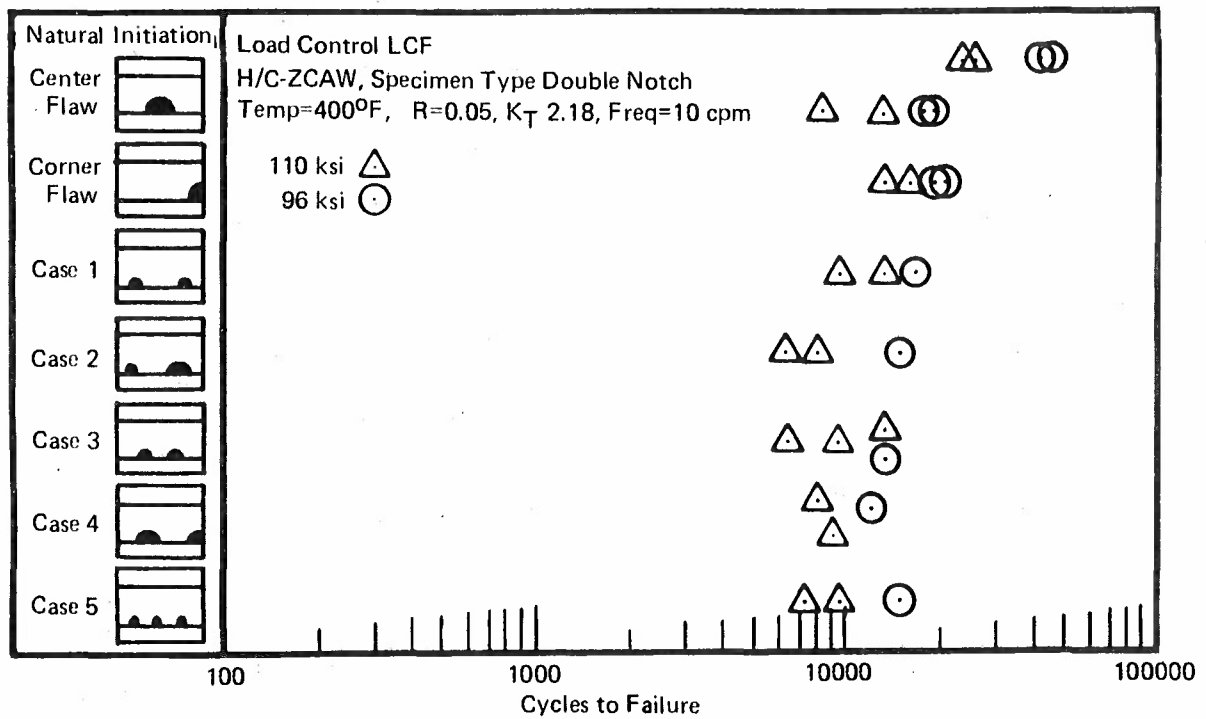
Figure 8.   Test Results for Waspaloy Double Notch Specimen

15
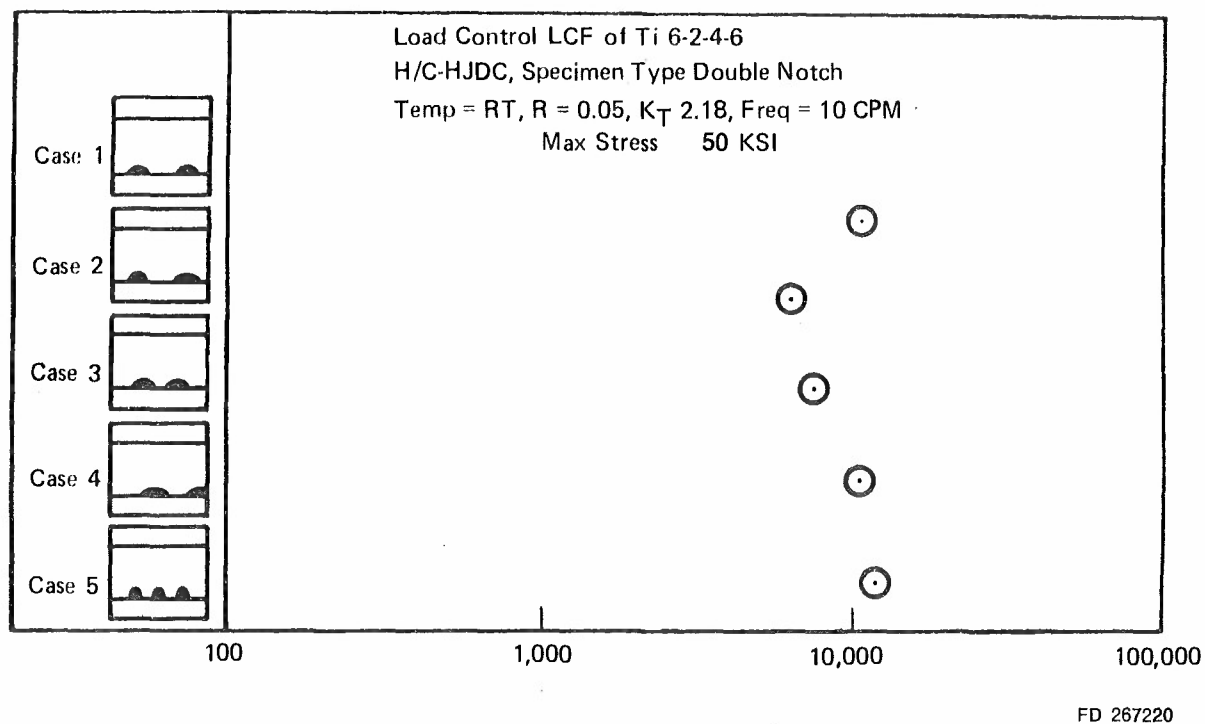
Figure 9. Test Results for Ti 6-2-4-6 Double Notch Specimen

Test Conditions:
Double Notch Specimen
110 KSI, R = 0.05
400°F, 10 CPM,

Fracture Surface Crack Dimensions

Total Cycle	Remaining Cycles	W	D	
0	—	0.022	0.026	Elox
3000	12,013	0.043	0.026	1st Heat
6000	9013	0.061	0.032	2nd Heat
10,000	5013	0.097	0.052	3rd Heat
15,013	—	0.248	0.120	Failure

Dimensions Only
Drawing Not To Scale
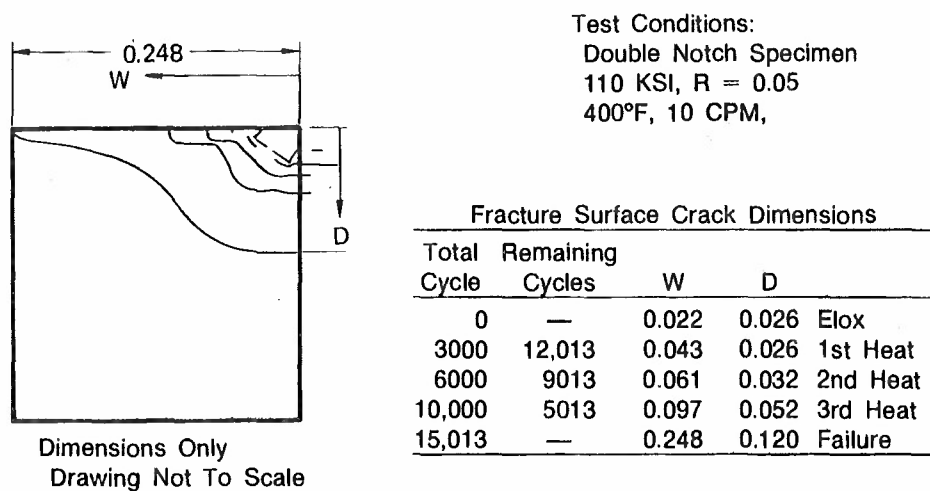
FD 267221

Figure 10. Fracture Surface Crack Contour Schematic for Waspaloy Singular Initiation Specimen No. 10, Corner Flaw
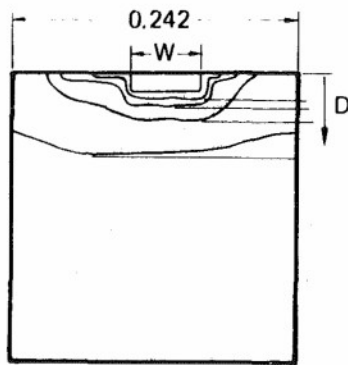
16

Fracture Surface Crack Dimensions

Total Cycle	Remaining Cycles	W	D	
0	—	0.038	0.020	Elox
2000	5336	0.0685	0.022	1st Heat
5000	2336	0.120	0.028	2nd Heat
6000	1336	0.190	0.048	3rd Heat
7336	—	0.242	0.110	Failure

Dimensions Only
Drawing Not To Scale.

FD 267222

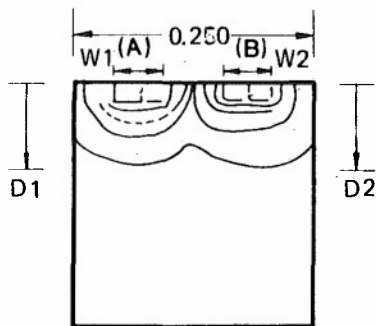*Figure 11. Fracture Surface Crack Contour Schematic for Waspaloy Singular Initiation Specimen No. 8, Center Flaw*

Fracture Surface Crack Dimensions

Total Cycle	Remaining Cycles	A		B		
		W1	D1	W2	D2	
0	—	0.040	0.010	0.040	0.012	Elox
3500	5806	0.057	0.011	0.062	0.013	1st Heat
7000	2306	0.085	0.019	0.086	0.021	2nd Heat
8000	1306	0.101	0.035	0.114	0.037	3rd Heat
9306	—	0.120	0.110	0.120	0.090	Failure

Dimensions Only
Drawing Not To Scale.

FD 267223

Figure 12. Fracture Surface Crack Contour Schematic for Waspaloy Multiple Initiation Specimen No. 18, Case 1

.17

Test Conditions:
Double Notch Specimen
110 KSI, R = 0.05
400°F, 10 CPM

Fracture Surface Crack Dimensions

Total Cycle	Remaining Cycles	W1	D1	W2	D2	
0	—	0.040	0.016	0.040	0.015	Elox
2000	6022	0.064	0.017	0.060	0.016	1st Heat
5000	3022	0.080	0.024	0.075	0.022	2nd Heat
6000	2022	0.096	0.041	0.102	0.037	3rd Heat
8022	—	0.122	0.100	0.122	0.070	Failure

FD 267224

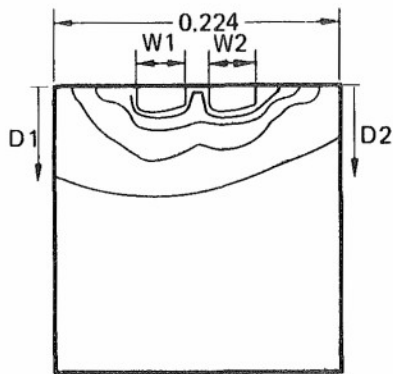Figure 13. *Fracture Surface Crack Contour Schematic for Waspaloy Multiple Initiation Specimen No. 3A, Case 2*

Test Conditions:
Double Notch Specimen
110 KSI, R = 0.05
400°F, 10 CPM

Fracture Surface Crack Dimension

Total Cycle	Remaining Cycles	W1	D1	W2	D2	
0	—	0.040	0.017	0.055	0.015	Elox
4000	2430	0.048	0.018	0.059	0.018	1st Heat
5000	1430	0.105	0.032	0.119	0.031	2nd Heat
6000	430	0.114	0.060	0.127	0.055	3rd Heat
6430	—	0.114	0.112	0.127	0.110	Failure

FD 267225

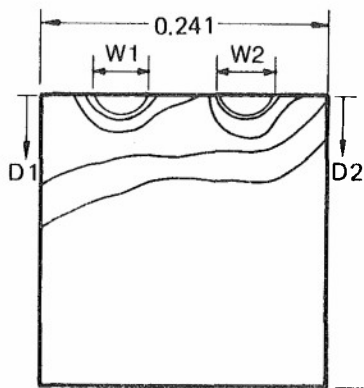Figure 14. *Fracture Surface Crack Contour Schematic for Waspaloy Multiple Initiation Specimen No. 9A, Case 3*
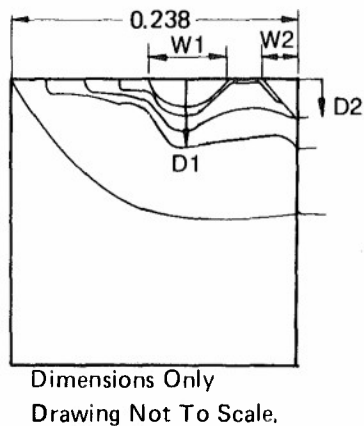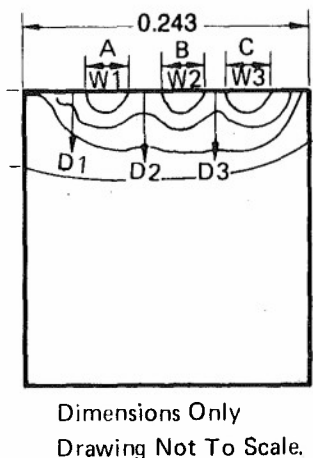
18

Test Conditions:
Double Notch Specimen
110 KSI, R = 0.05
400°F, 10 CPM

Fracture Surface Crack Dimensions

Total Cycle	Remaining Cycles	W1	D1	W2	D2	
0	—	0.035	0.019	0.014	0.019	Elox
2000	6853	0.052	0.020	0.021	0.019	1st Heat
5000	3853	0.066	0.027	0.021	0.031	2nd Heat
6000	2853	0.118	0.049	0.021	0.047	3rd Heat
8853	—	0.119	0.120	0.119	0.120	Failure

Dimensions Only
Drawing Not To Scale.

FD 267226

Figure 15. Fracture Surface Crack Contour Schematic for Waspaloy Multiple Initiation Specimen No. 14A, Case 4

Test Conditions:
Double Notch
Specimen 110 KSI
400°F, 10 CPM.

Fracture Surface Crack Dimensions

Total Cycle	Remaining Cycles	A		B		C		
		W1	D1	W2	D2	W3	D3	
0	—	0.019	0.008	0.018	0.009	0.018	0.010	Elox
5000	2352	0.053	0.018	0.059	0.024	0.060	0.025	1st Heat
6000	1352	0.093	0.023	0.059	0.039	0.067	0.032	2nd Heat
7352	—	0.093	0.100	0.075	0.110	0.050	0.050	Failure

Dimensions Only
Drawing Not To Scale.

FD 267227

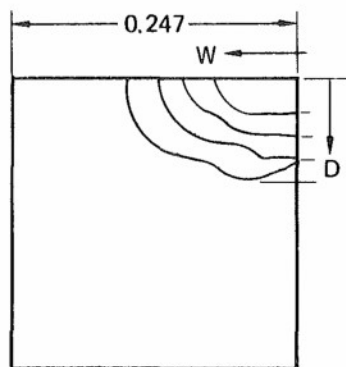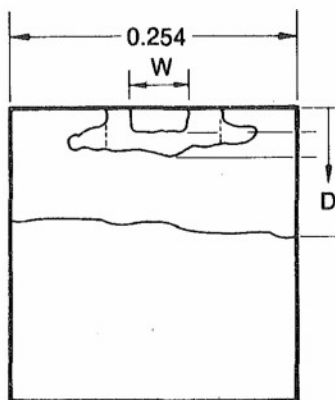*Figure 16. Fracture Surface Crack Contour Schematic for Waspaloy Multiple Initiation Specimen No. 19A, Case 5*

19

Test Conditions:
Double Notch Specimen
92 KSI, R = 0.05
75°F, 10 CPM

Fracture Surface Crack Dimensions

Total Cycles	Remaining Cycles	W	D	
0	—	0.040	0.017	Elox
1500	1107	0.049	0.027	1st Heat
2100	507	0.054	0.040	2nd Heat
2200	407	0.066	0.067	3rd Heat
2607	—	0.247	0.242	Failure

Dimensions Only
Drawing Not To Scale

FD 267228

Figure 17. Fracture Surface Crack Contour Schematic for Ti 6-2-4-6 Single Initiation Specimen No. 6B, Corner Flaw

Test Conditions:
Double Notch Specimen
92 KSI, R = 0.05
75°F, 10 CPM

Fracture Surface Crack Dimensions

Cycles	Remaining Cycles	W	D	
0	—	0.040	0.019	Elox
500	09	0.072	0.066	1st Heat
509	—	0.254	0.120	Failure

Dimensions Only
Drawing Not To Scale

FD 267229

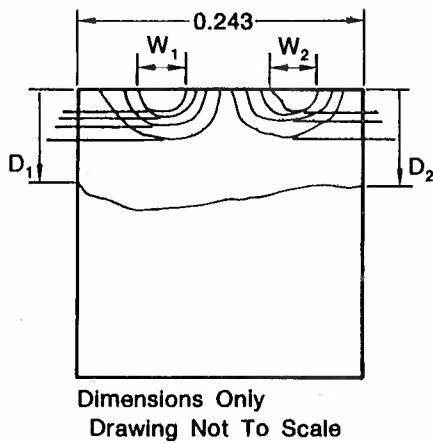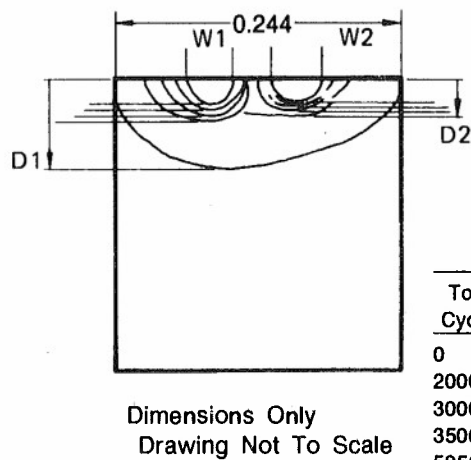*Figure 18. Fracture Surface Crack Contour Schematic for Ti 6-2-4-6 Single Initiation Specimen No. 4B, Center Flaw*

20

2014C

Figure 19. *Fracture Surface Crack Contour Schematic for Ti 6-2-4-6 Multiple Initiation Specimen No. 8B, Case 1*

Test Conditions:
Double Notch Specimen
50 ksi, R = 0.05
75°F, 10 cpm

Fracture Surface Crack Dimensions

Total Cycle	Remaining Cycles	W1	D1	W2	D2	
0	—	0.040	0.014	0.040	0.014	Elox
4000	5987	0.042	0.015	0.0415	0.014	1st Heat
5000	4987	0.043	0.017	0.0445	0.016	2nd Heat
9000	987	0.095	0.027	0.0685	0.036	3rd Heat
9987	—	0.1215	0.090	0.1215	0.050	Failure

FD 267230

Figure 20. *Fracture Surface Crack Contour Schematic for Ti 6-2-4-6 Multiple Initiation Specimen No. 10B, Case 2*
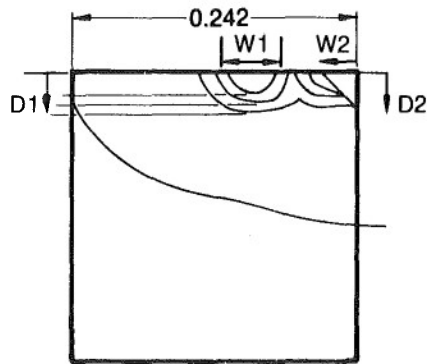
Test Conditions:
Double Notch Specimen
50 KSI, R = 0.05
75°F, 10 CPM

Fracture Surface Crack Dimensions

Total Cycles	Remaining Cycles	W1	D1	W2	D2	
0	—	0.048	0.020	0.048	0.015	Elox
2000	3958	0.059	0.021	0.054	0.016	1st Heat
3000	2958	0.066	0.022	0.061	0.017	2nd Heat
3500	2458	0.074	0.027	0.065	0.024	3rd Heat
5958	—	0.122	0.070	0.122	0.070	Failure

FD 267231

21

Test Conditions:
Double Notch Specimen
50 KSI, R = 0.05
75°F, 10 CPM

Dimensions Only
Drawing Not To Scale

Fracture Surface Crack Dimensions

Total Cycles	Remaining Cycles	W2	D2	W1	D1	
0	—	0.018	0.020	0.039	0.014	Elox
4500	7420	0.024	0.020	0.039	0.014	1st Heat
6400	5520	0.029	0.020	0.044	0.021	2nd Heat
8500	3420	0.0355	0.020	0.0685	0.028	3rd Heat
11,920	—	0.121	0.120	0.121	0.120	Failure

FD 267232

Figure 21.   Fracture Surface Crack Contour Schematic for Ti 6-2-4-6 Multiple Initiation Specimen No. 12B, Case 3

Test Conditions:
Double Notch Specimen
50 KSI, R = 0.05
75°F, 10 CPM

Dimensions Only
Drawing Not To Scale

Fracture Surface Crack Dimensions

Total Cycles	Remaining Cycles	W1	D1	W2	D2	
0	—	0.041	0.014	0.060	0.015	Elox
2000	5091	0.045	0.017	0.065	0.019	1st Heat
5000	2091	0.064	0.025	0.081	0.029	2nd Heat
6000	1091	0.081	0.030	0.098	0.036	3rd Heat
7091	—	0.1225	0.150	0.1225	0.150	Failure

FD 267233

Figure 22.   Fracture Surface Crack Contour Schematic for Ti 6-2-4-6 Multiple Initiation Specimen No. 14B, Case 4
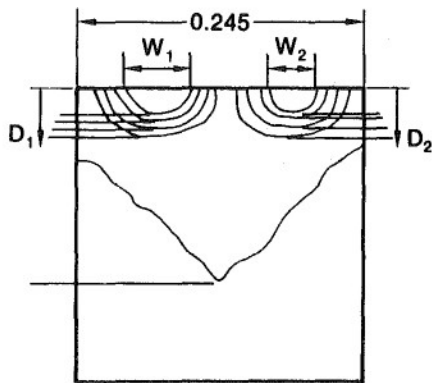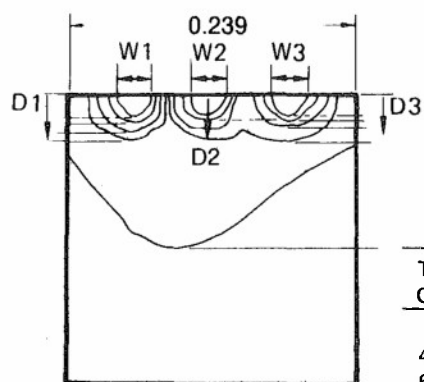
22

Test Conditions:
Double Notch Specimen
50 KSI, R = 0.05
75°F, 10 CPM

Fracture Surface Crack Dimensions

Total Cycle	Remaining Cycles	W1	D1	W2	D2	W3	D3	
0	—	0.020	0.010	0.020	0.011	0.020	0.011	Elox
4000	7167	0.022	0.012	0.023	0.012	0.022	0.012	1st Heat
6500	4667	0.029	0.014	0.033	0.014	0.027	0.015	2nd Heat
8500	2667	0.053	0.018	0.055	0.018	0.037	0.019	3rd Heat
11,167	—	0.0796	0.150	0.0796	0.150	0.0796	0.150	Failure

Dimensions Only
Drawing Not To Scale

FD 267234

Figure 23.   Fracture Surface Crack Contour Schematic for Ti 6-2-4-6 Multiple Initiation Specimen No. 16B, Case 5

23

CRACK GROWTH ANALYSIS

GENERAL

The analytical treatment included crack growth life predictions performed in three ways:

1. As singular cracks

2. As multiple cracks using an existing P&W part-through crack prediction program with a modification to the stress intensity parameter to account for multiple cracks

3. As multiple cracks using a multiple-degree-of-freedom model developed by a consultant specifically for prediction of multiple crack behavior.

These analyses had several common elements. The crack growth rate predictions were based on the standard Pratt & Whitney Hyperbolic Sine (SINH) models for the materials. This method for representing crack growth rate data as a function of temperature, frequency, and stress ratio has been successfully used on a number of gas turbine and other materials (References 4 through 10). Source of the raw da/dN versus ΔK data was ASTM standard test specimens which were tested in accordance with ASTM E 647, Standard Test Method For Constant-Load-Amplitude Fatigue Crack Growth Rates Above 10^{-8}m/Cycle. The basic da/dN versus ΔK curves were the same for all analysis for each material. Stress intensity versus crack size relationships for the double notch specimen were based on handbook solutions (Reference 11) except for alterations made for multiple crack analyses.

The primary consideration in comparing singular and multiple crack behavior for RFC purposes is the effect on actual and predicted life. A trial case was evaluated for the double-edge notch specimen to compare calculated lives for single and multiple cracks. For the trial case, remaining lives for both corner and surface flaws were predicted to represent singular cracks. The worst possible case of multiple cracking was presumed to be a through crack of uniform depth. At the conditions selected, little or no difference in remaining life was predicted for the two singular crack conditions, but a 50 to 90 percent decrease in life was predicted for through-crack of the same initial depth. Actual and predicted lives for the multiple crack cases were expected to fall between these extremes. Single crack predictions for all three cases and remaining life results for both single and multiple crack cases in both materials are presented in Figures 24 through 27.

MODIFIED CRACK GROWTH PREDICTIONS

The initial analytical effort was to model and predict the crack growth life of notched specimens containing multiple cracks using current fracture mechanics-based methodology. The basic life prediction model, used for singular and multiple occurring flaw shapes/geometries, was a P&W model developed for part through crack predictions at stress concentration regions. This program, shown schematically in Figure 28, provides mission mix capability and built-in interpolative crack growth models for the most common gas turbine materials. For local stress concentration regions, this partial-through (surface) crack life prediction program uses a root mean square (RMS) value of stress intensity (K) to simulate the complex K which actually varies along the entire crack surface. A two degrees-of-freedom model accurately represents the more complex multi-degrees-of-freedom three-dimensional cracking problems through use of influence function theory.
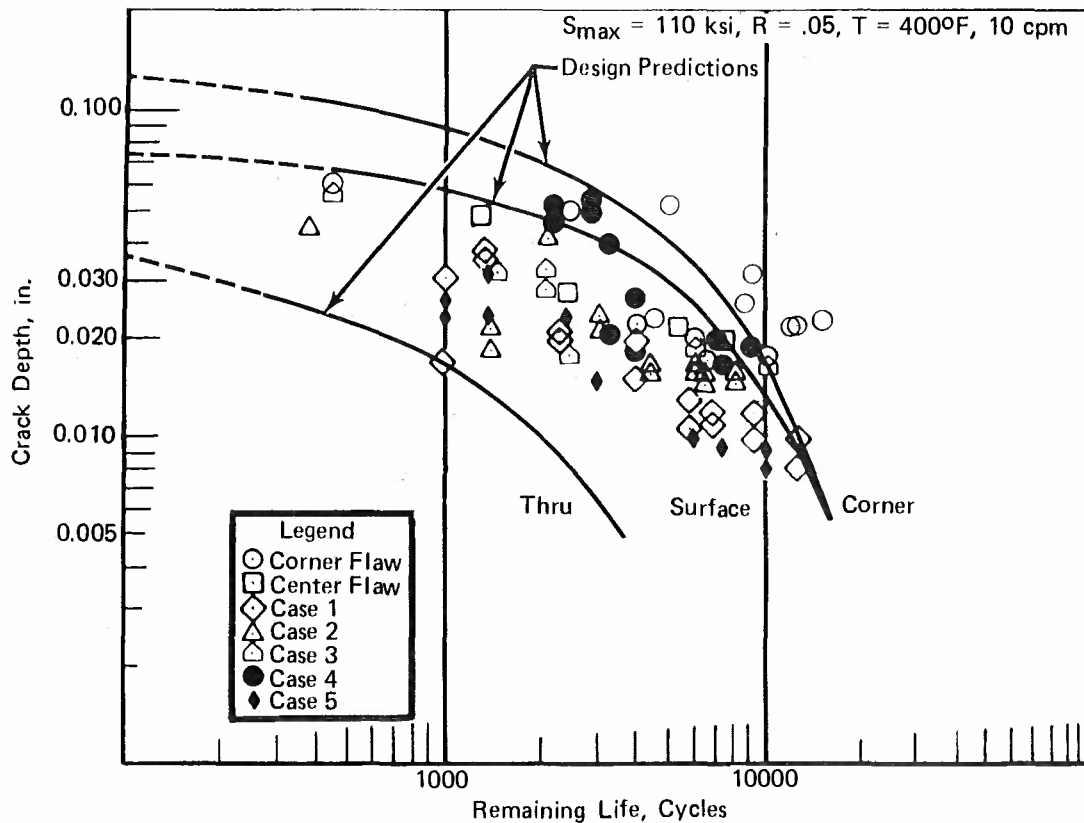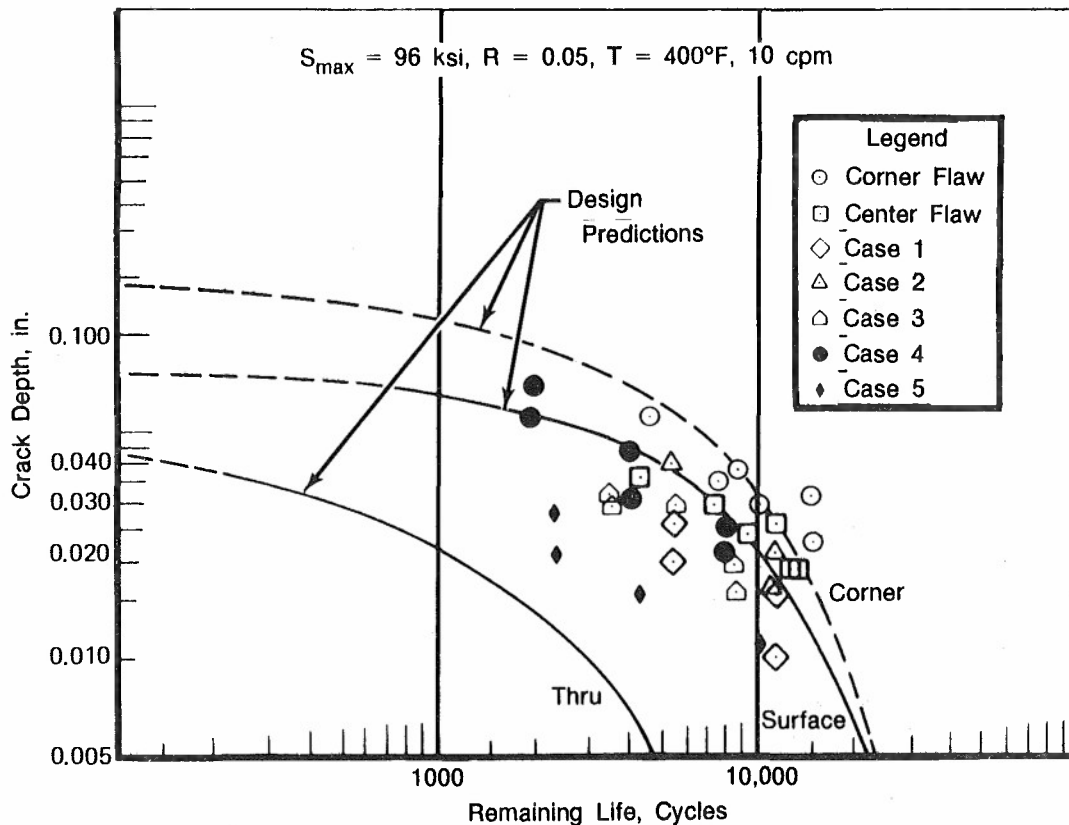
Figure 24.   Life Remaining Cycles Versus Crack Depth for Waspaloy; High Stress Condition

For the singular occurring flaw shapes tested in this task, the life prediction model described above was adequate. However, to analyze the multiple crack initiation (MCI) cases, the prediction methodology described above was modified as outlined in Figure 29. The empirical formula depicted in Figure 30 was used in step three in Figure 29 to recalculate the change in stress intensity factor at the crack tips, as the single colinear cracks propagated toward one another.

The crack prediction methodology outlined in Figure 29 applies where symmetric cracks can be assumed (cases 2 and 5). For MCI cases 1, 3, and 4, either a non-symmetric condition existed initially (case 4, corner/surface flaw combination), or developed as a result of an EDM surface flaw(s) progressing to a corner crack before linking with the adjacent crack. To account for this non-symmetry in the prediction methodology, a corner crack model was substituted in step three and propagated for one or both cracks as the situation required. After determining at what cycle link-up occurred, the cracks were modeled and cycled to failure.

A comparison of the fracture mechanics predictions and the laboratory test results for Waspaloy with single through cracks and multiple crack indications are presented in the form of probability distribution plots in Figures 31 and 32, respectively. For the single part through cracks in Waspaloy, the typical actual/predicted (a/p) ratio is conservative by about 40 percent, with no ratio greater than 4.0 or less than 0.5 (i.e., B50 to B.1 scatter is approximately 2.0 on life). For MCI in Waspaloy, the typical a/p ratio is conservative by approximately 52 percent, with no ratio greater than 4.0 or less than 0.6 (i.e., overall B50 to B.1 scatter is approximately 2.0). These results compare very well with the prediction accuracy observed in the single crack cases (i.e., the scatter factor for both is approximately 2.0).

25

Figure 25. *Life Remaining Cycles Versus Crack Depth for Waspaloy; Low Stress Condition*

FD 267236

For multiple crack indications in Ti 6-2-4-6, the comparison of predictions and test results are summarized in the probability distribution plot shown in Figure 33. The typical a/p ratio is conservatively biased by approximately 42 percent. Data scatter (B50/B.1) is approximately 1.55 with no a/p greater than 2.5 or less than 0.8.

MULTIPLE-DEGREE-OF-FREEDOM MODEL

While current fracture mechanics methodology was being employed by P&W to predict crack growth for this task, Dr. A. F. Grandt, Jr., of Purdue University, was retained to investigate alternate techniques for predicting the behavior of multiple cracks. His approach used a multi-degree-of-freedom computer program to predict the initial growth coalescence, and ultimate fracture of the remaining dominant crack.

The approach and results are described in more detail by Tritsch and Grandt (References 12 and 13). Using this method, stress intensity factors are determined at the crack tip locations as indicated by the numbers in Figure 34. Corresponding crack growth rates were then calculated for each location, and the cycles for a small crack extension were computed for one of the locations. Subsequently, the crack extension for each of the other locations was calculated for the same number of cycles. This procedure was then iterated, allowing the cracks to progress naturally until crack tips contacted either a free surface or another flaw. At this point, instantaneous transition to another uniform surface, corner, or through thickness flaw shape was assumed to encompass the boundaries of the now connected flaws. The analysis was continued until predicted fracture.
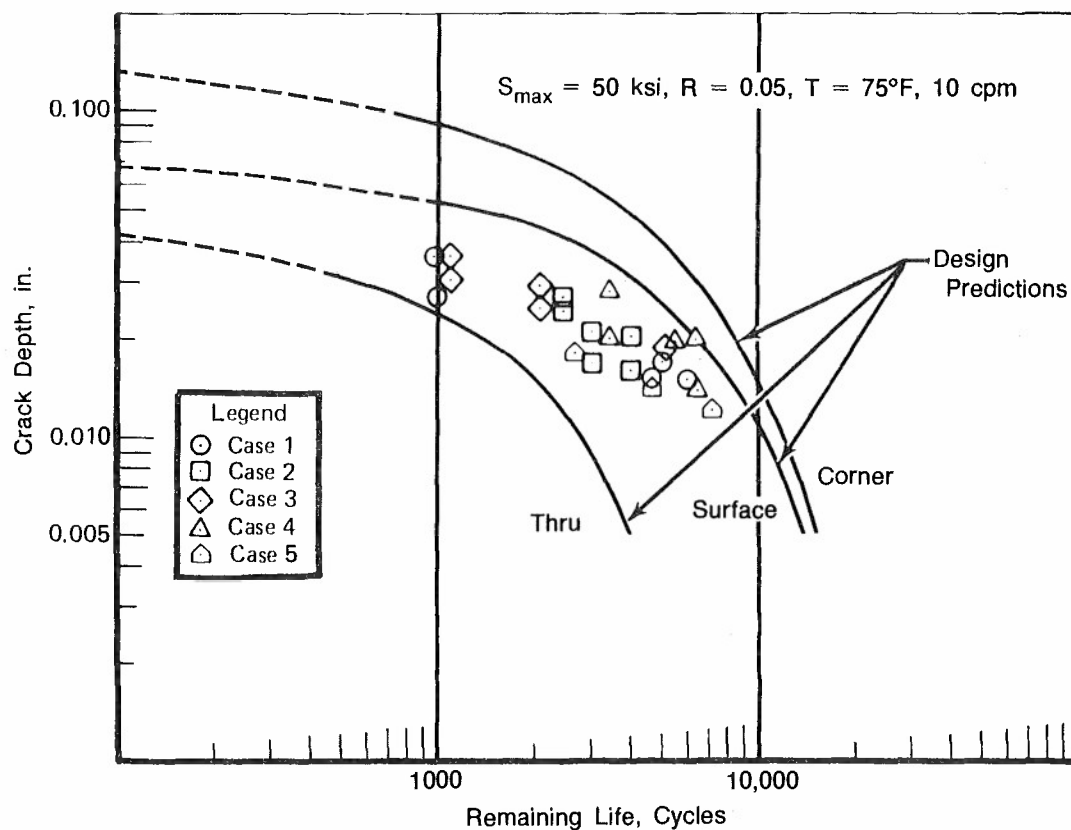
26
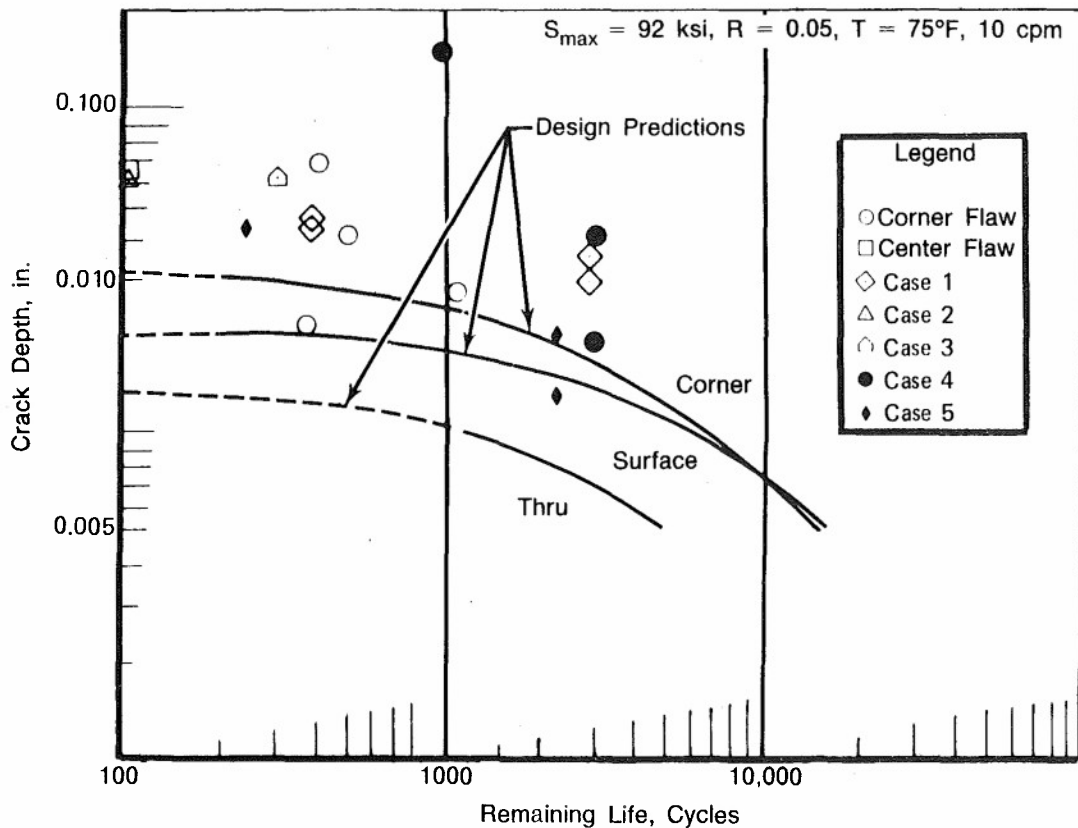
Figure 26. *Life Remaining Cycles Versus Crack Depth for Ti 6-2-4-6; High Stress Condition*

Computations of crack tip stress intensities were based on solutions by Newman and Raju (Reference 14) for single surface and corner flaws. These flaws were modified both for the double-edge notch specimen geometry and to add an interaction factor to increase the effective stress intensity for adjacent, interacting cracks.

The same crack length data generated in this task for Waspaloy and Ti 6-2-4-6 was input to the program. Predictions were based on the first observed fatigue crack as the initial flaw size. Probability distributions comparing the predicted versus actual lives for Waspaloy and Ti 6-2-4-6 are presented in Figures 35 and 36.

Variability in predictions with the multiple-degree-of-freedom model was slightly less than using the previous technique. Some of the predictions were anticonservative, and in general the predictions were less conservative than for the modified design technique. These results are discussed more fully by Brandt, Thakker, and Tritsch (Reference 15).
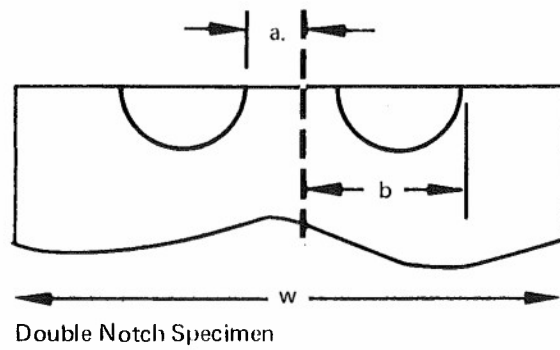
27

$S_{max} = 50$ ksi, $R = 0.05$, $T = 75°F$, 10 cpm

Legend
⊙ Case 1
▢ Case 2
◇ Case 3
△ Case 4
⬠ Case 5

Design Predictions

Thru Surface Corner

FD 267238

Figure 27. Life Remaining Cycles Versus Crack Depth for Ti 6-2-4-6; Low Stress Condition
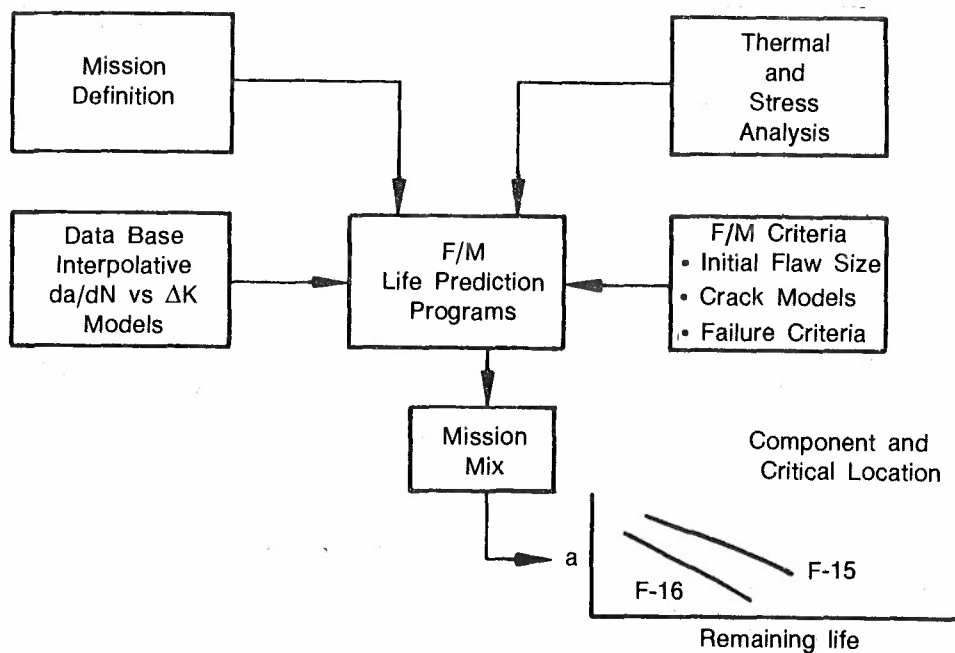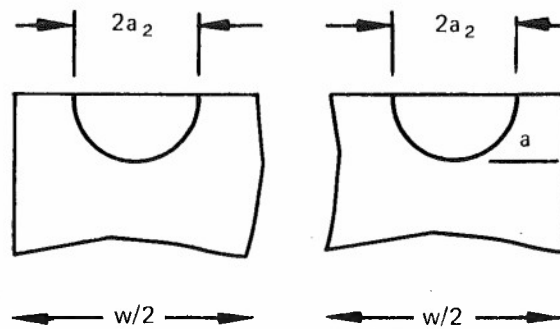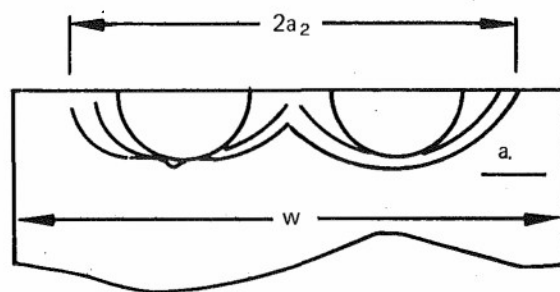

FD 267239

Figure 28. F/M Prediction Schematic

28

I   Multiple Crack Initiation
Specimen with
Nearly Symmetric
Crack Sizes

Double Notch Specimen

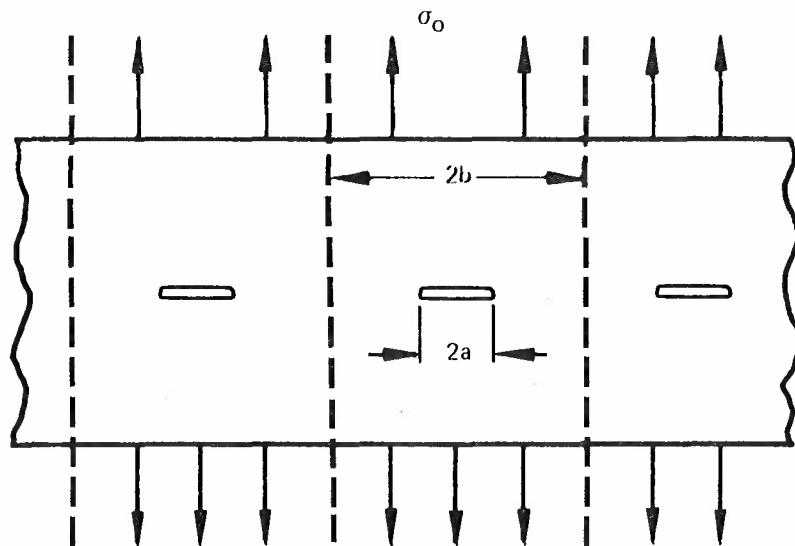II   MCI Specimen is
Modeled as Two
Separate Cracks

III   At Crack Edge, Stress
Intensity is
Recalculated to Reflect
Cracks Propagating
Toward One Another

K_I Recalc

IV   Having Determined
Cycles at Which
Cracks Have Linked-Up,
Large Aspect Ratio
Crack is Modeled
and Cycled to Failure

FD 267240

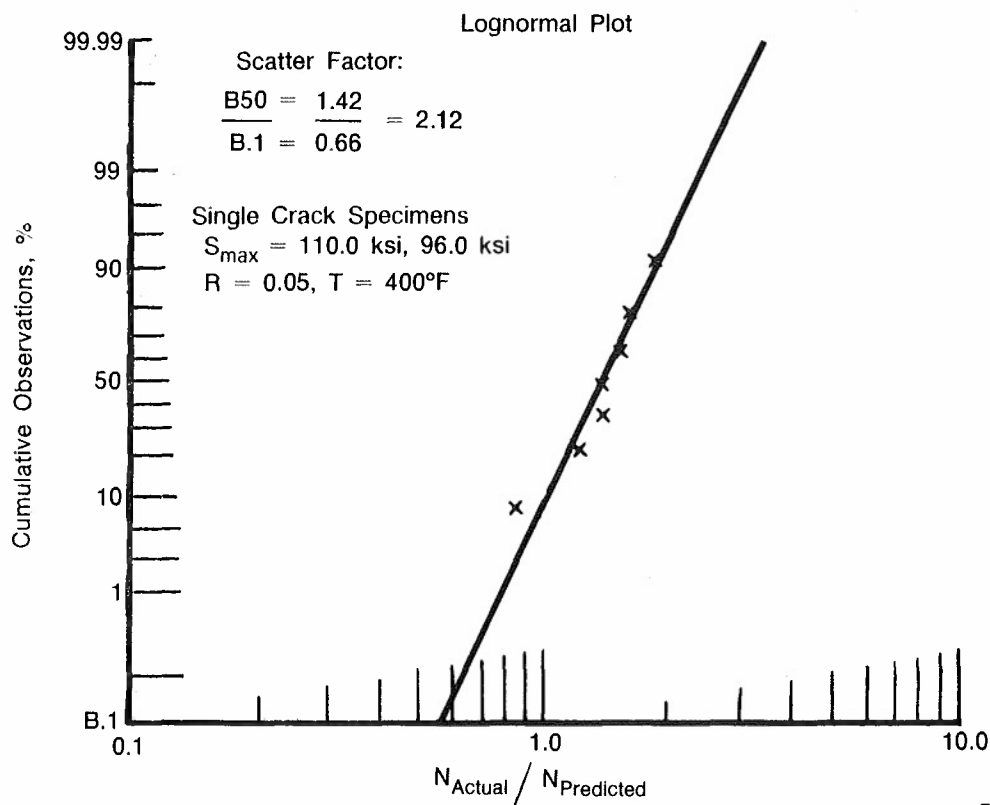Figure 29. Modified Crack Growth Prediction Methodology

29

$$K_1 = \sigma_o \sqrt{\pi a} \left(\frac{2b}{\pi a} \tan \frac{\pi a}{2b} \right)^{1/2}$$

$$K_2 = 0$$

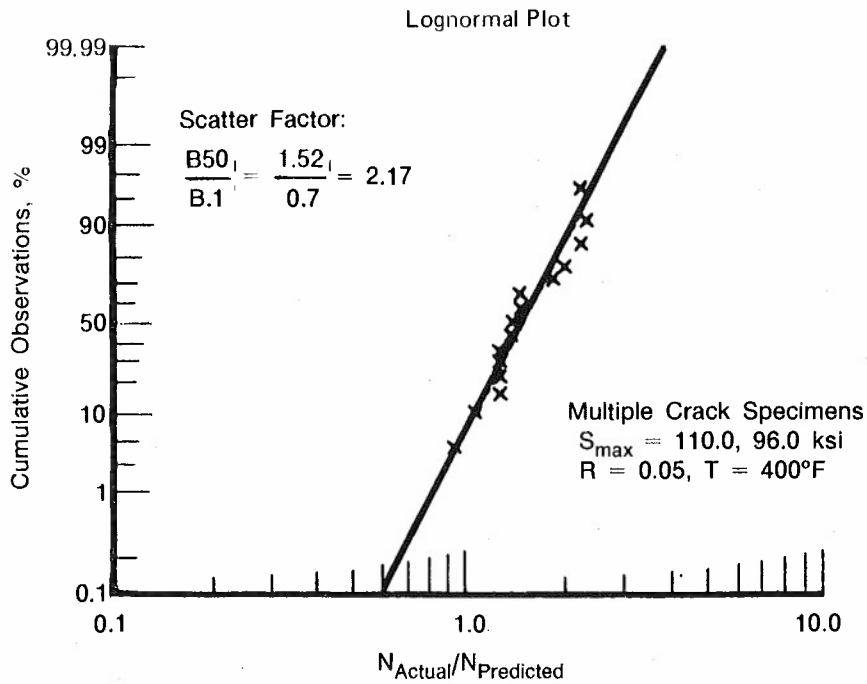(This solution was taken from Paris and Tada " Fracture Mechanics Handbook".)

FD 267241

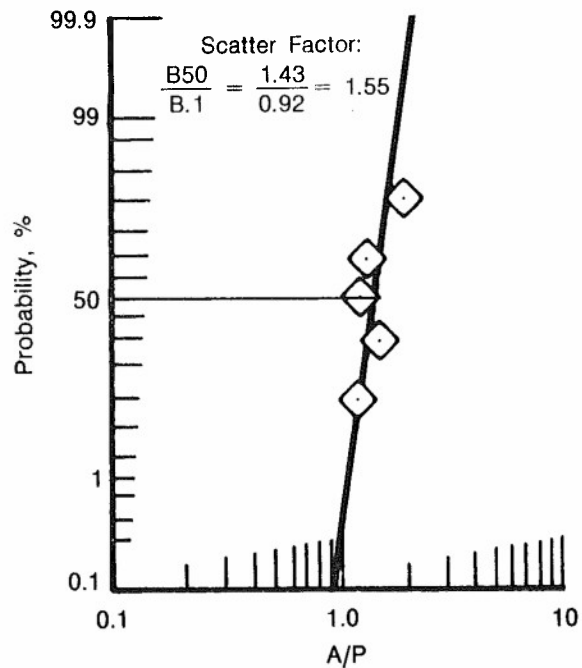*Figure 30.* *Plate With a Periodic Array of Colinear Cracks Under Uniform Stress at Infinity*

FD 267242

Figure 31. *Waspaloy Double Notch Specimens — Distribution of Actual/Predicted Life Ratios; Single Crack Specimens*
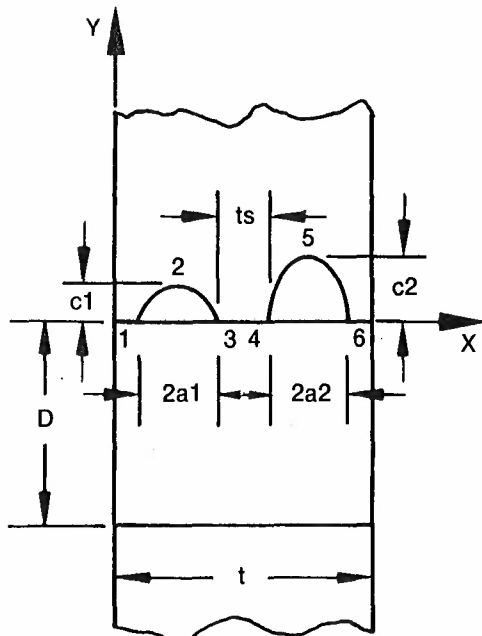
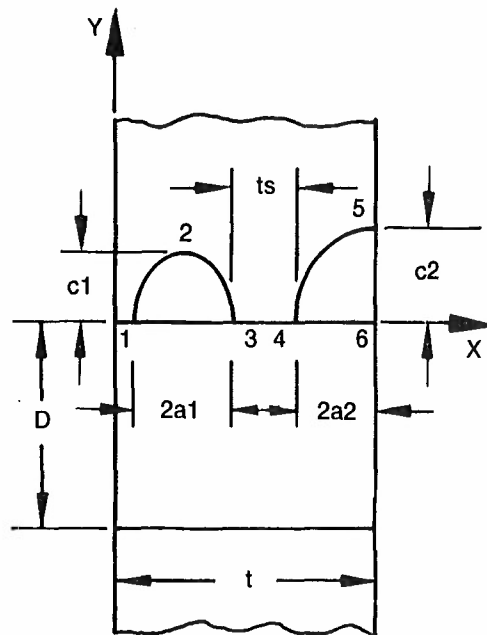Figure 32. *Waspaloy Double Notch Specimens — Distribution of Actual/Predicted Life Ratios; Multiple Crack Specimens*
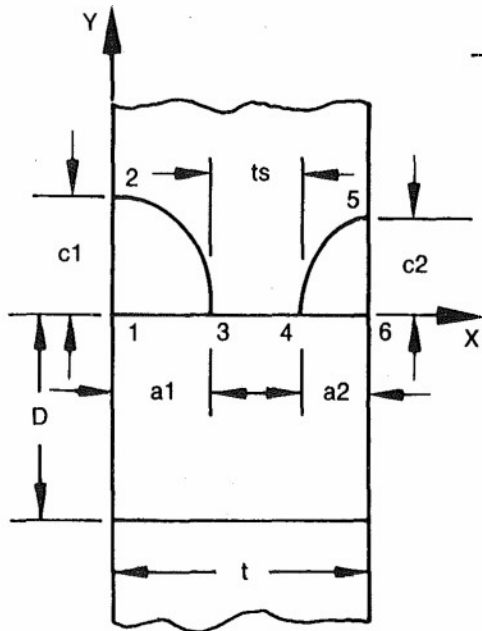

Figure 33. *Multiple Crack Initiation Probability Distribution for Ti 6-2-4-6*

a. Two Surface Cracks

b. Surface and Corner Crack
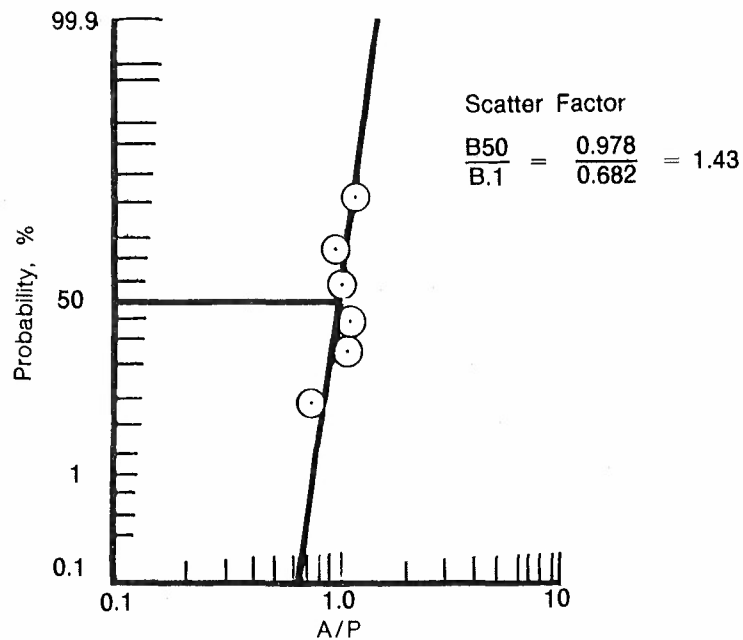
c. Two Corner Cracks

Hole diameter is D, plate thickness is t, and remote tensile stress is applied in z direction.

FD 283905

Figure 34. Schematic of Multiple Cracks Located Along Bore of a Hole in a Large Plate

32

Scatter Factor

$$\frac{B50}{B.1} = \frac{0.978}{0.682} = 1.43$$

FD 267245

Figure 35. Waspaloy Double Notch Specimen Distribution of Actual/Predicted Life Ratios by Multidegree of Freedom Prediction Method

Scatter Factor:

$$\frac{B50}{B.1} = \frac{0.741}{0.286} = 2.59$$
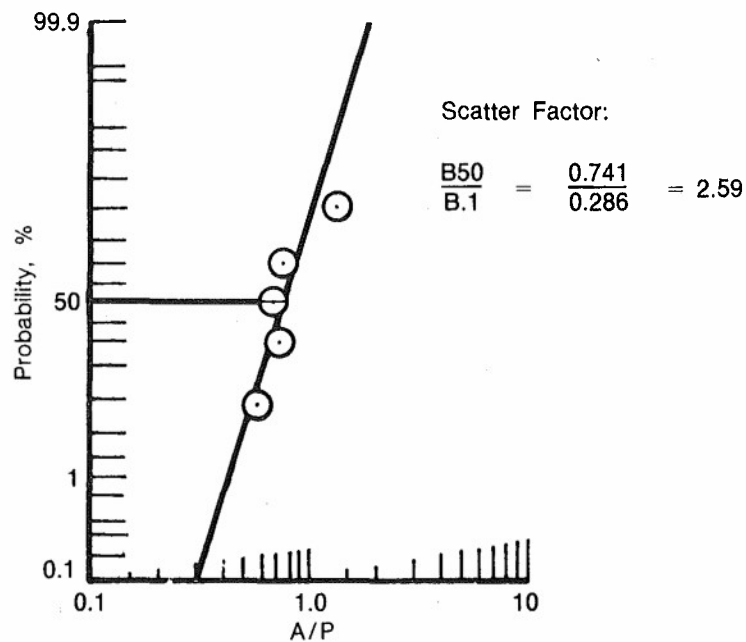
FD 267246

Figure 36. Ti 6-4-2-6 Double Notch Specimen Distribution of Actual/Predicted Life Ratios by Multidegree of Freedom Prediction Method

SECTION VI

CONCLUSIONS

The purpose of this task was to investigate the current life prediction methodology for multiple crack growth in gas turbine engine components. To this end, the experimental and analytical efforts described above were carried out. Current prediction methods for very small cracks (as small as 0.005 × 0.010 inches) were modified to address the larger interacting cracks produced by the controlled preflaw methods used in this program. Results using the modified procedure are summarized in the following conclusions:

1. The modified crack growth life prediction technique currently in use resulted in acceptable but conservative predictions in all cases. Variability in the predictions was also acceptable, and was similar to variability in predicted versus actual results for singular crack cases.

2. The multiple-degree-of-freedom approach also produced acceptable life predictions, and in fact demonstrated reduced variability in predicted versus actual results. It was, however, more complicated to use and did not result in a consistent conservative bias in the life predictions.

3. Based on this study, the modified crack growth life prediction technique currently in use is considered adequate for Retirement-for-Cause applications. The multiple-degree-of-freedom approach offers potential improvements for future use.

SECTION VII

REFERENCES

1. Hill, R., W. Reimann, J. Ogg, "A Retirement for Cause Study of an Engine Turbine Disk," AFWAL-TR-81-2094, November 1981.

2. Harris, J., D. Sims, C. Annis, Jr., "Concept Definition: Retirement for Cause of F100 Rotor Components," AFWAL-TR-80-4188, September 1980.

3. Annis, C. G., Jr., VanWanderham, J. A. Harris, Jr., and D. L. Sims, "Gas Turbine Engine Disk Retirement-for-Cause: An Application of Fracture Mechanics and NDE," ASME Publication 8-GT-127, ASME Gas Turbine Conference, New Orleans, Louisiana, March 10-13, 1980.

4. Annis, C. G., R. M. Wallace, and D. L. Sims, "An Interpolative Model for Elevated Temperature Fatigue Crack Propagation," AFML-TR-76-176, Part I, November 1976, presented at 1977 SESA Spring Meeting, Dallas, TX, May 1977.

5. Wallace, R. M., C. G. Annis, and D. L. Sims, "Application of Fracture Mechanics at Elevated Temperatures," AFML-TR-76-176, Part II, November 1976, presented to Air Force Materials Laboratory, WPAFB, OH May 1977.

6. Sims, D. L., C. G. Annis, and R. M. Wallace, "Cumulative Damage Fracture Mechanics at Elevated Temperature," AFML-TR-76-176, Part III, November 1976.

7. Sims, D. L., "Evaluation of Crack Growth in Advanced P/M Alloys," AFML-TR-79-4160, September 1979.

8. Larsen, J. M., C. G. Annis, Jr., "Observation of Crack Retardation Resulting from Load Sequencing Characteristic of Military Gas Turbine Operation," presented at ASTM Symposium on Effects of Load Spectrum Variables on Fatigue Crack Initiation and Propagation, San Francisco, CA, May 1979.

9. Larsen, J. M., B. J. Schwartz, C. G. Annis, Jr., "Cumulative Damage Fracture Mechanics Under Engine Spectra," AFML-TR-79-4159, September 1979.

10. Annis, C. G., Jr., "An Engineering Approach to Cumulative Damage Fracture Mechanics in Gas Turbine Disks," presented at ASME Gas Turbine Conference, San Diego, CA, March 1979.

11. Tada, H., P. C. Paris, and G. R. Irwin, "The Stress Analysis of Cracks Handbook," Del Research Corporation, Hellertown, PA, 1973.

12. Tritsch, D. E., "Prediction of Fatigue Crack Lives and Shapes," M. S. Thesis, School of Aeronautics and Astronautics, Purdue University, W. Lafayette, Indiana, August 1983.

13. Grandt, A. F., Jr., "Fatigue Life Predictions for Multiple Cracked Notches," Memorandum Report to A. B. Thakker, School of Aeronautics and Astronautics, Purdue University, W. Lafayette, Indiana, May 1983.

14. Newman, J. C., and I.S. Raju, "Stress-Intensity Factor Equations for Cracks in Three-Dimensional Finite Bodies," *NASA Technical Memorandum 83200,* NASA Langley Research Center, Hampton, Virginia, August 1981.

15. Grandt, A. F., Jr., A. B. Thakker, and D. E. Tritsch, "An Experimental and Numerical Investigation of the Growth and Coalescence of Multiple Fatigue Cracks at Notches," ASTM 17th National Symposium on Fracture Mechanics, Albany, New York, August 7-9, 1984.

201·IC